The Insulated Linear Antenna—Revisited

Thorsten W. Hertel, *Student Member, IEEE* and Glenn S. Smith, *Fellow, IEEE*

***Abstract*—In the past, the insulated linear antenna has been analyzed with an approximate transmission-line theory. The range of validity for this theory has not been established. In this paper, the finite-difference time-domain (FDTD) method is used to analyze the insulated monopole antenna. The validity of the FDTD analysis is established by comparison of results with accurate measurements for a variety of antennas. The FDTD analysis is then used to determine the accuracy of the approximate transmission-line theory. Graphs are provided to quantify the errors in the approximate theory as functions of the geometry and the electrical properties of the monopole antenna.**

***Index Terms*—FDTD, insulated antennas, transmission-line theory.**

I. Introduction

An insulated antenna is formed by placing a simple wire antenna such as a dipole or loop in a dielectric sheath such as a plastic tube. Insulated antennas are almost always used in an ambient medium, such as soil, seawater, or biological tissue, whose electrical properties are quite different from those of the insulation. Fig. 1 shows an insulated monopole antenna. This is a vertical metal rod of height h and radius a placed over a metal image plane. It is fed through the image plane by a coaxial line with inner and outer radii a and b, respectively. The cylindrical insulation of height h_i and radius $b_i > a$ extends beyond the top end of the metal rod. The insulation is assumed to be a lossless dielectric with relative permittivity ϵ_{ri} and the external medium has the relative permittivity ϵ_{re} and the conductivity σ_e. Both media are assumed to be nonmagnetic $\mu = \mu_\circ$.

Insulated antennas were apparently first proposed for use in highly conducting media. For example, as early as 1919 insulated loops were used as low-frequency communication antennas on submarine boats in seawater [1]–[3]. When the external medium is highly conducting, it is clear that the monopole antenna shown in Fig. 1 can be modeled as a coaxial line with the rod forming the inner conductor and the external medium forming the lossy outer conductor. Conventional transmission-line formulas are then easily adapted to provide a useful analysis of this antenna [4]–[6].

In the early 1970's, R.W.P. King and his coworkers at Harvard University discovered that the external medium did not have to be highly conducting for the transmission-line model to be useful for the insulated linear antenna. All that was required was

Manuscript received February 11, 1999; revised April 4, 2000. This work was supported in part by the Joint Services Electronics Program under Contract DAAH-04-96-1-0161.

The authors are with the School of Electrical and Computer Engineering, Georgia Institute of Technology, Atlanta, GA 30332-0250 USA (email: hertel@ece.gatech.edu; glenn.smith@ece.gatech.edu).

Publisher Item Identifier S 0018-926X(00)05797-5.

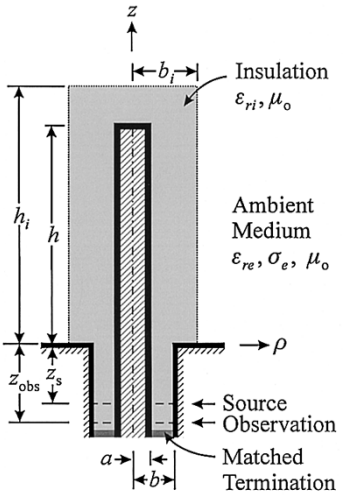

Fig. 1. Model for the insulated monopole antenna.

that the wavenumber in the external medium be much larger than that in the insulation, specifically

$$|k_e/k_i|^2 \gg 1 \tag{1}$$

where the complex wavenumber is

$$k = \beta - j\alpha = \frac{\omega}{c}\sqrt{\epsilon_r - j\frac{\sigma}{\omega\epsilon_\circ}} = k_\circ\sqrt{\epsilon_r}\sqrt{1 - jp} \tag{2}$$

and $p = \sigma/\omega\epsilon_\circ\epsilon_r$ is the loss tangent for an assumed $e^{j\omega t}$ time dependence. Notice that the external medium can even be a lossless dielectric in which case the inequality (1) becomes

$$\epsilon_{re}/\epsilon_{ri} \gg 1. \tag{3}$$

The insulated monopole antenna shown in Fig. 1 can be viewed as a section of coaxial transmission-line terminated in an open circuit. The current in the antenna (center conductor of the line) is then

$$I(z) = \frac{jV_\circ}{Z_c}\frac{\sin[k_L(h-z)]}{\cos(k_L h)} \tag{4}$$

where the complex wavenumber k_L and characteristic impedance Z_c for the transmission line are

$$\begin{aligned} k_L &= \beta_L - j\alpha_L \\ &= k_i\sqrt{\frac{k_e^2\left[H_0^{(2)}(k_e b) + k_e b\,\ln(b/a)H_1^{(2)}(k_e b)\right]}{k_i^2 H_0^{(2)}(k_e b) + k_e^2 k_e b\,\ln(b/a)H_1^{(2)}(k_e b)}} \end{aligned} \tag{5}$$

and

$$Z_c = \frac{\eta_i k_L}{2\pi k_i}\left(\ln(b/a) + \frac{k_i^2}{k_e^2}\frac{H_0^{(2)}(k_e b)}{k_e b\,H_1^{(2)}(k_e b)}\right). \tag{6}$$

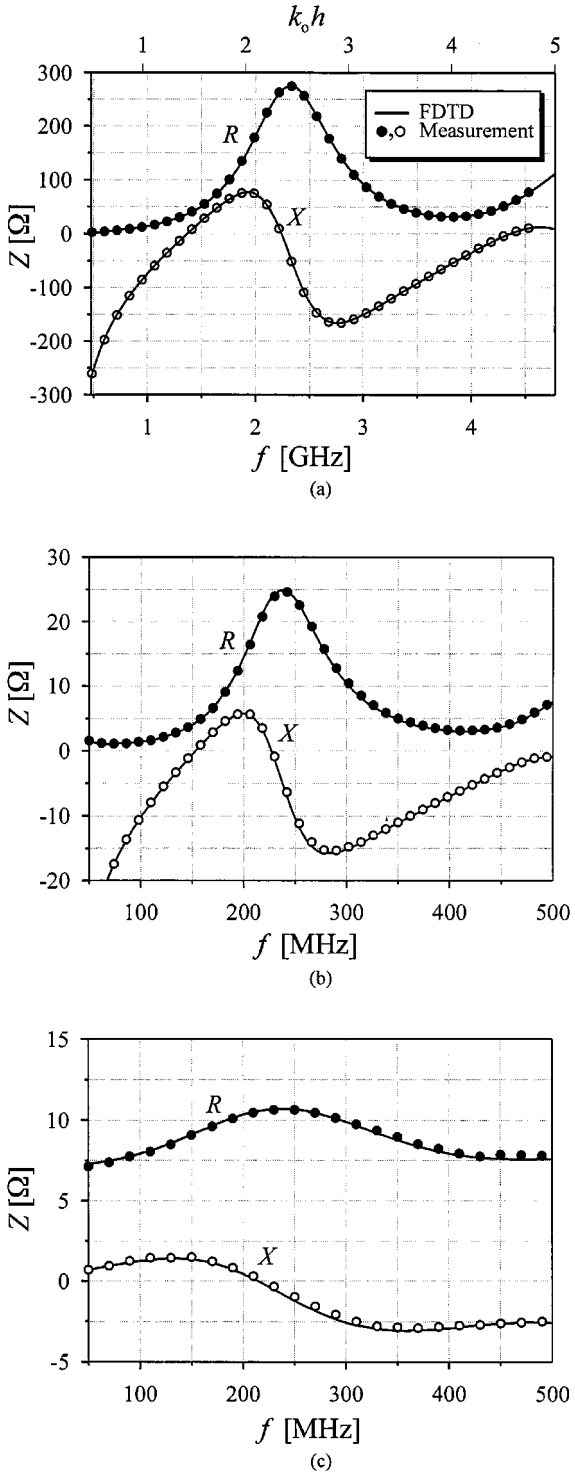

Fig. 2. Comparison of FDTD results with Scott's measurements [16] for the input impedance of bare monopole antennas in (a) air, (b) fresh water, and (c) salt water.

In these expressions, $H_n^{(2)}$ is a Hankel function of order n. The input impedance of the monopole antenna is obtained from the ratio of the voltage $V_\circ$ to the current at the drive point $(z = 0)$ (4); that is

$$Z = R + jX = -jZ_c \cot(k_L h). \tag{7}$$

King's group at Harvard went on to make extensive theoretical and experimental studies for a variety of insulated antennas, e.g., eccentrically insulated monopoles, coupled insulated monopoles, and insulated loops. Much of this research is summarized in [7]. More recently, insulated antennas have been tailored for specific applications such as for the treatment of cancer using microwave hyperthermia [8]–[10].

An interesting question with regard to the use of the transmission-line theory for the insulated antenna is, "How well does the inequality, (1), or (3) for lossless media, have to be satisfied for the theory to provide accurate results?" In [7], various quantitative interpretations for this inequality were offered. Of course, some indication of the accuracy was obtained from comparisons with experimental results. However, the experiments were for limited values of the electrical parameters of the insulation and external medium. In addition, some of the measurements were made on monopole antennas that did not correspond precisely to the simple geometry shown in Fig. 1. For example, dielectric tubes were sometimes used to contain the material forming the insulation, air gaps existed between the conductor and the solid insulation, and dielectric supports were placed in the external medium to properly align and hold the insulation. Also, these early measurements were made without the use of a network analyzer, so the accuracy is lower than commonly obtained today.

In this paper, the insulated monopole antenna shown in Fig. 1 is accurately analyzed using the finite-difference time-domain (FDTD) method, and the results from this analysis are used to answer the question posed above. In Section II of this paper, the details of the FDTD method as applied to this antenna are briefly described, and in Section III, the validity of the analysis is established by comparing calculated results with a number of new experimental measurements. In Section IV, parametric studies are presented that compare the predictions of the transmission-line theory with the FDTD results for a wide range of geometrical and electrical properties of the antenna. The results of these comparisons are summarized in a set of graphs that show the percentage error to be expected when the transmission-line theory is used for the insulated monopole antenna.

II. Antenna Analysis

In this section, the FDTD analysis for the insulated linear monopole antenna shown in Fig. 1 is briefly described. The FDTD method is inherently a time-domain technique, so the analysis is performed using a pulsed excitation. Fourier transformation is then used to obtain frequency-domain results, e.g., the input impedance for comparison with the transmission-line theory.

The dimensions of the coaxial line feeding the antenna (a, b) are chosen so that only the TEM mode propagates within the line at the frequencies of interest. The incident voltage $\mathcal{V}_{\rm inc}(t)$ excites the antenna at the source plane. When the distance z_s from this plane to the junction between the coaxial line and the antenna is chosen so that $z_s > (b - a)$, the fields of all modes higher than the TEM, which are generated at the junction, are insignificant at the source plane. The source is configured to produce an outgoing TEM wave above the source plane and a negligible field below; this device is referred to as a "one-way

TABLE I
PARAMETERS OF FRESH WATER AND SALT WATER

Measurement	T	$\epsilon_{r\infty}$	ϵ_{r0}	σ_0	τ
Bare Ant., Fresh Water	22.0°C	4.90	79.4	$8.00 \cdot 10^{-3}$ S/m	$8.77 \cdot 10^{-12}$s
Bare Ant., Salt Water	22.0°C	4.90	78.0	1.00 S/m	$8.76 \cdot 10^{-12}$s
Ins. Ant., Fresh Water	22.7°C	4.90	79.2	$8.00 \cdot 10^{-3}$ S/m	$8.62 \cdot 10^{-12}$s

injector" [11], [12]. Thus, only the reflected voltage $\mathcal{V}_{\rm ref}(t)$ is present at the observation plane $z_{\rm obs}$, which is below the source plane.

For this study, the incident voltage is the differentiated Gaussian pulse

$$\mathcal{V}_{\rm inc}(t) = V_\circ(t/\tau_p)e^{0.5-0.5(t/\tau_p)^2} \tag{8}$$

with the Fourier transform

$$V_{\rm inc}(\omega) = \mathcal{F}\{\mathcal{V}_{\rm inc}(t)\} = -jV_\circ\sqrt{2\pi}\,\tau_p(\omega\tau_p)e^{0.5-0.5(\omega\tau_p)^2}. \tag{9}$$

The characteristic time for the pulse $\tau_p = 1/\omega_\circ$ determines the useful spectrum for this signal. The spectrum exceeds ten percent of its peak value when ω is within the range $0.06\omega_\circ < \omega < 2.8\omega_\circ$ (the 10% bandwidth). The differentiated Gaussian pulse has a well-defined spectral peak and a small low-frequency content. The latter property is a desirable feature for the FDTD analysis, because significant low-frequency content in the exciting pulse can lead to unacceptably long settling times.

The Fourier transforms of the incident and reflected voltages are used to calculate the reflection coefficient

$$\Gamma(z_{\rm obs}, \omega) = \frac{V_{\rm ref}(z_{\rm obs}, \omega)}{V_{\rm inc}(z_{\rm obs}, \omega)} = \frac{\mathcal{F}\{\mathcal{V}_{\rm ref}(z_{\rm obs}, t)\}}{\mathcal{F}\{\mathcal{V}_{\rm inc}(z_{\rm obs}, t)\}} \tag{10}$$

and the impedance

$$Z_{\rm obs} = Z(z_{\rm obs}, \omega) = Z_{ci}\,\frac{1+\Gamma(z_{\rm obs}, \omega)}{1-\Gamma(z_{\rm obs}, \omega)} \tag{11}$$

at the observation plane. Here, Z_{ci} is the characteristic impedance of the feeding coaxial line, which is filled with the same material as the insulation:

$$Z_{ci} = \frac{\eta_i}{2\pi}\,\ln(b/a) = \frac{1}{2\pi}\sqrt{\frac{\mu_\circ}{\epsilon_\circ\epsilon_{ri}}}\,\ln(b/a). \tag{12}$$

The "apparent impedance" Z of the monopole antenna at the image plane is obtained by transforming the impedance at the observation plane over the distance $z_{\rm obs}$

$$Z = R + jX = Z_{ci}\,\frac{Z_{\rm obs} + jZ_{ci}\,\tan(k_i z_{\rm obs})}{Z_{ci} + jZ_{\rm obs}\,\tan(k_i z_{\rm obs})}. \tag{13}$$

This is the ideal impedance that when placed at the end of the coaxial line (propagating only TEM waves) produces the same reflection coefficient at the observation plane as the monopole antenna [7].

The rotational symmetry of the antenna and excitation allow an analysis in the two spatial coordinates ρ and z. The finite two-dimensional discretized domain for the FDTD analysis is truncated with the new perfectly matched layer (PML) absorbing boundary condition for cylindrical coordinates [13]. This PML almost totally absorbs all outgoing electromagnetic waves in the external medium. An extensive investigation of the PML used in this study shows that it reflects less than 0.1% of a wave incident on its surface [14]. Typically, dimensions of the FDTD cells were $\Delta\rho \approx \Delta z = a/3$. Using the conventional Courant number for two dimensions, i.e., $\Delta t = \Delta\rho\sqrt{\epsilon_{ri}}/2c$, $2 \cdot 10^4$ timesteps were usually sufficient to obtain convergence.

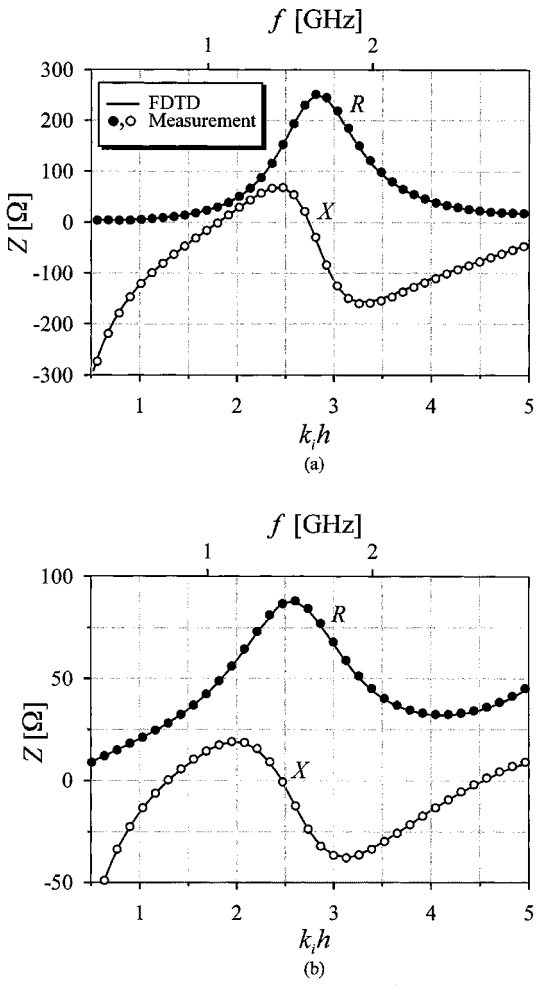

Fig. 3. Comparison of FDTD results with measurements for the input impedance of monopole antennas with Teflon insulation in (a) air and (b) fresh water.

In some of the comparisons with measurements to be presented in the following section, the external medium is a saline solution. The electrical properties of this medium exhibit dispersion over the range of frequencies of interest, and this dispersion must be accounted for in the theoretical analysis. In the analysis, the saline solution is modeled as a dielectric material

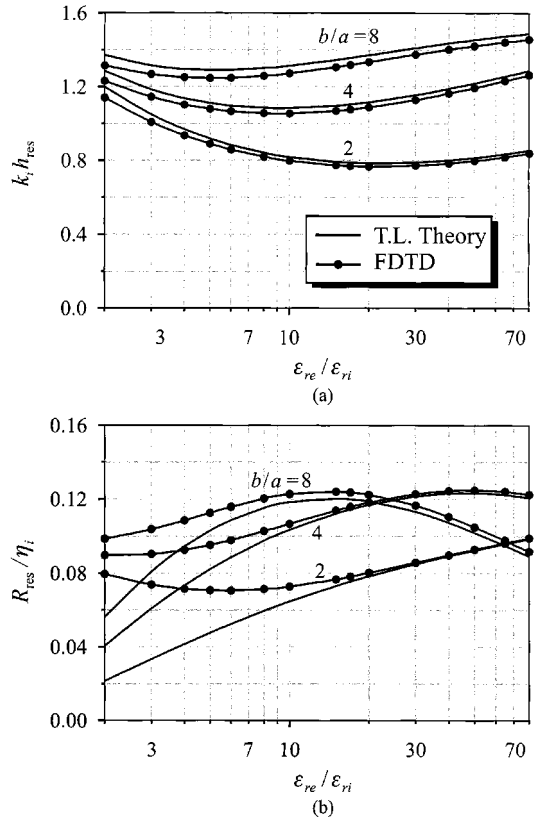

Fig. 4. Comparison of (a) the resonant height $k_i h_{\rm res}$ and (b) the resistance at resonance $R_{\rm res}/\eta_i$ for the transmission-line theory (solid line) with FDTD calculations (solid line with dots). The external medium is lossless.

with a single Debye relaxation [7], [14]. The effective relative permittivity and effective conductivity of the medium are then

$$\epsilon_{re}(\omega) = \epsilon_{r\infty} + \frac{\epsilon_{r0} - \epsilon_{r\infty}}{1 + (\omega\tau)^2} \tag{14}$$

and

$$\sigma_e(\omega) = \sigma_0 + \frac{\epsilon_{r0} - \epsilon_{r\infty}}{1 + (\omega\tau)^2}\ \omega^2 \tau \epsilon_0. \tag{15}$$

In these equations, ϵ_{r0} is the low-frequency relative permittivity, $\epsilon_{r\infty}$ is the high-frequency relative permittivity, τ is the relaxation time, and σ_0 is the low-frequency conductivity. All of these parameters are functions of the normality and the temperature of the saline solution, and they must be determined from empirically derived expressions [7], [15].

The dispersion was incorporated in the FDTD computations in the following manner. The frequency range of interest was divided into several small segments; a typical segment was centered at ω_i and of width $\Delta\omega_i$. The computation was performed using a pulse with characteristic time $\tau_{pi} = 1/\omega_i$ and the electrical properties given by (14) and (15) with $\omega = \omega_i$. The results from the computation were then used to obtain the impedance over the small segment $\Delta\omega_i$. The segments were chosen small enough that no discernable differences were observed for the impedances at the ends of adjacent segments.

III. Validation of FDTD Analysis: Measurements

The FDTD analysis described in the previous section will be used as the standard when determining the range of validity

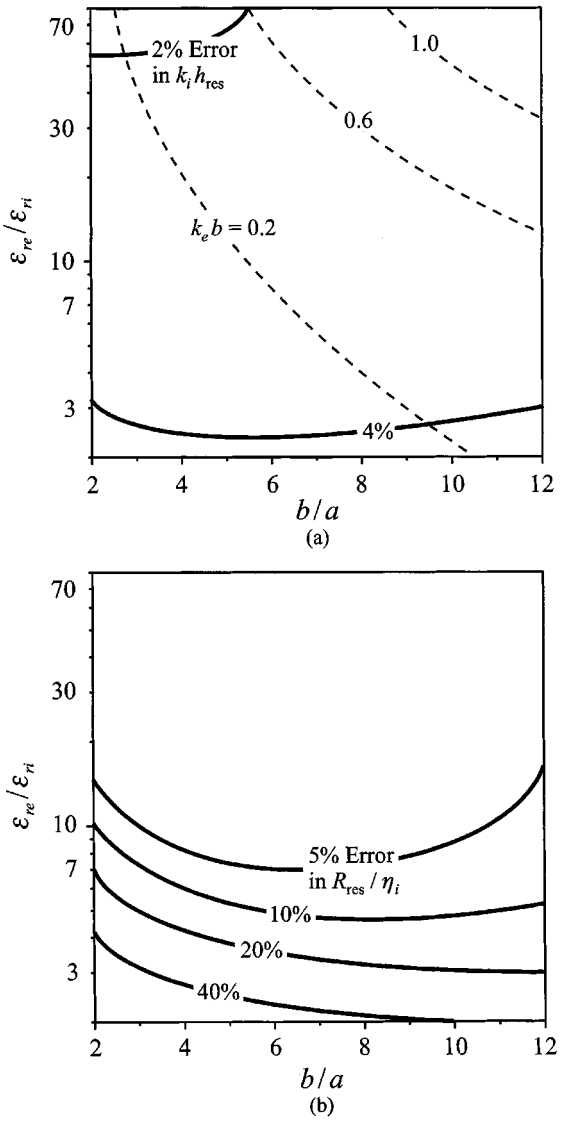

Fig. 5. Contour plot of the error in (a) the resonant height $k_i h_{\rm res}$ and (b) the resistance at resonance $R_{\rm res}/\eta_i$ as a function of $\epsilon_{re}/\epsilon_{ri}$ and b/a for a lossless external medium. Lines of constant $k_e b$ are dashed on this graph.

for the approximate transmission-line model for the insulated linear antenna. Thus, it is very important that the accuracy of the FDTD analysis be firmly established. This is done by a thorough comparison of the FDTD results with accurate measurements made on model antennas with the geometry shown in Fig. 1. The full details of the measurement procedure are described in reference [14]; only the results will be presented here.

The first set of results, shown in Fig. 2, are for a bare monopole and use measurements made by W. R. Scott, Jr. [16]. For these results, the length-to-radius ratio for the monopole is $h/a = 32.9$, and the air-filled coaxial line feeding the antenna has $b/a = 2.30$ (precision 7-mm line, with characteristic impedance $Z_c = 50.0\ \Omega$). Results are presented for three different materials surrounding the monopole: Fig. 2(a) air, (b) fresh water, and (c) salt water. The electrical parameters for the last two materials are given in Table I. The apparent impedances shown in Fig. 2(b) and (c) are referenced to a

point in the transmission line slightly below the image plane $z/h = -0.04$.

For all three cases, the agreement between the FDTD theoretical results (solid line) and the measurements (solid and open dots) is very good. The small difference that can be seen in the reactances in Fig. 2(c) is possibly due to the inaccuracy associated with measuring an impedance that is severely mismatched to the characteristic impedance of the transmission line [16]. For this case, the reflection coefficient is typically $|\Gamma| > 0.65$ with $|\angle\Gamma - \pi| < 7°$. Notice that these results cover an extreme range of electrical parameters for the surrounding medium. The relative permittivity for Fig. 2(b) is nearly 80 times that for Fig. 2(a). This causes the resonant frequency (where $X = 0$) and the resistance at resonance both to drop by nearly a factor of ten. The conductivity for Fig. 2(c) is nearly 100 times that for Fig. 2b. This causes the resonance almost to disappear.

The second set of results, shown in Fig. 3, are for an insulated monopole. For these results, the length-to-radius ratio for the monopole is $h/a = 37.4$. The insulation is formed from Teflon with the dimensions $h_i/a = 44.1$ and $b_i/a = 2.97$. The relative permittivity of this Teflon, which was measured by W. R. Humbert, is $\epsilon_{ri} = 2.04$ [17]. The Teflon filled coaxial line feeding the antenna has $b/a = 2.30$ (precision 7-mm line, with characteristic impedance $Z_{ci} = 35.0\ \Omega$).

Fig. 3(a) is for the insulated monopole in air, while Fig. 3(b) is for the insulated monopole in fresh water with the electrical properties given in Table I. For both cases, the agreement between the FDTD theoretical results (solid line) and the measurements (solid and open dots) is very good. These two cases again represent extremes. For Fig. 3(a), the relative permittivity for the external medium is about a factor of two lower than that of the insulation, whereas for Fig. 3(b), the relative permittivity for the external medium is about a factor of 40 higher than that of the insulation. Note that the first case Fig. 3(a) is one for which the transmission-line model would not apply since the inequality (1) is clearly violated.

IV. Range of Validity for the Transmission-Line Model

In this section, results computed from the approximate transmission-line model for the insulated monopole antenna will be compared with accurate numerical calculations made with the FDTD method. These comparisons will lead to a better understanding of the range of validity for the transmission-line model, specifically, the degree to which the inequality (1) must be satisfied for the model to be used.

There are a number of quantities that could be used for the comparison. At first glance, the complex wavenumber k_L (5) seems a likely candidate for the comparison since it plays a key role in the transmission-line model. However, this quantity has no precise meaning for an antenna, so any attempt to extract it from the FDTD results would introduce additional approximations. After some thought, the quantities selected for the comparison are the electrical height $k_i h_{\rm res}$ of the antenna at the first resonance of the impedance and the normalized resistance at this resonance $R_{\rm res}/\eta_i$. These quantities are examined as functions of the relative thickness of the insulation b_i/a and the ratio of

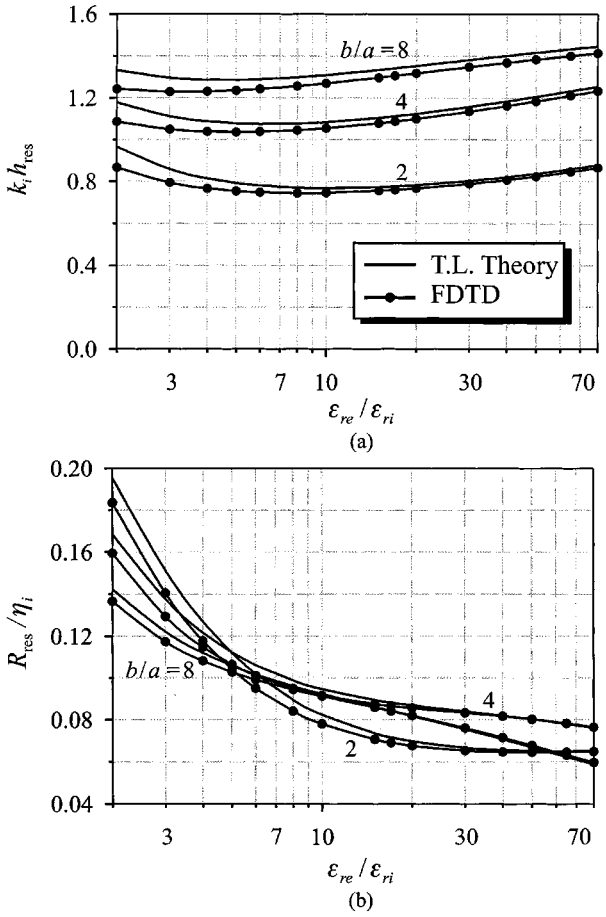

Fig. 6. Comparison of (a) the resonant height $k_i h_{\rm res}$ and (b) the resistance at resonance $R_{\rm res}/\eta_i$ for the transmission-line theory (solid line) with FDTD calculations (solid line with dots). The external medium is lossy $p_e(\omega_{\rm res}) = 1.0$.

the permittivity of the external medium to that of the insulation $\epsilon_{re}/\epsilon_{ri}$. The height of the antenna relative to its radius is held fixed at $h/a = 100$, the outer radius of the coaxial feed line is equal to that of the insulation $b = b_i$, and the height of the insulation is $h_i = h + 3b$ in all of the comparisons.

The results in Fig. 4 are for a lossless external medium (conductivity $\sigma_e = 0$) for which the inequality in (1) becomes $\epsilon_{re}/\epsilon_{ri} \gg 1$. The resonant height and resistance at resonance are shown as functions of the ratio of permittivities $\epsilon_{re}/\epsilon_{ri}$ for three different sizes of the insulation $b/a = 2$, 4, and 8. The resonant height predicted by the transmission line model is seen to agree favorably with the FDTD results even when the inequality $\epsilon_{re}/\epsilon_{ri} \gg 1$ does not hold. Specifically, for the extreme case $\epsilon_{re}/\epsilon_{ri} = 2$, the results for the transmission-line model are only in error by about 5% for any of the values of b/a. The resistance at resonance predicted by the transmission-line model, however, is seen to deviate from the FDTD results whenever $\epsilon_{re}/\epsilon_{ri} < 15$. The deviation is slightly greater for the smallest value of b/a.

The errors associated with the transmission-line model are quantified in Fig. 5. Here, the percentage errors in the electrical height [shown in Fig. 5(a)] and the resistance at resonance [shown in Fig. 5(b)] are shown as functions of the ratios $\epsilon_{re}/\epsilon_{ri}$ and b/a. These results are again for lossless media. Curves of

constant $k_e b$ are also shown in Fig. 5(a). This parameter is a measure of the electrical size of the insulation in the external medium.

In these figures, regions are marked where the error is less than a given percentage. The error in the resonant height is seen to be less than 5% for the entire graph: $2 \leq \epsilon_{re}/\epsilon_{ri} \leq 80$ and $2 \leq b/a \leq 12$. However, the error in the resistance at resonance is less than 5%, only when $\epsilon_{re}/\epsilon_{ri}$ is greater than about 15. The ratio b/a has a small effect on this error except near the extremes of b/a; that is, when $b/a \approx 2$ and 12. The highest errors occur, as expected, when both $\epsilon_{re}/\epsilon_{ri}$ and b/a are small (in the lower left-hand corner of the graph).

When the external medium is lossy (conductivity $\sigma_e \neq 0$), the ratio of wavenumbers in (1) becomes

$$|k_e/k_i|^2 = \left(\frac{\epsilon_{re}}{\epsilon_{ri}}\right)\sqrt{1+p_e^2(\omega)}. \tag{16}$$

For the comparison of results, it is convenient to fix the value of the loss tangent at a particular frequency. Notice from Fig. 4(a) that resonance for the insulated antenna occurs when $k_i h \approx \pi/2$ or for the frequency $\omega \approx \omega_{\rm res} = \pi c_i/2h$. When the loss tangent at this frequency is selected as a parameter; that is, $p_e(\omega_{\rm res}) = \sigma_e/\omega_{\rm res}\epsilon_o\epsilon_{re}$, (16) becomes

$$|k_e/k_i|^2 = \left(\frac{\epsilon_{re}}{\epsilon_{ri}}\right)\sqrt{1+\left(\frac{\pi p_e(\omega_{\rm res})}{2k_i h}\right)^2}. \tag{17}$$

For the results shown in Figs. 6 and 7, the value $p_e(\omega_{\rm res}) = 1.0$ is used. The addition of loss to the external medium is seen to change the resonant heights only slightly [compare Figs. 4(a) and 6(a)]. Hence, the errors in the resonant height for the transmission-line theory, Fig. 7(a), differ by only a few percent from those in the lossless case [Fig. 5(a)]. However, the resistances at resonance are now quite different [compare Figs. 3(b) and 6(b)]. The addition of loss has greatly improved the agreement between the transmission-line theory and FDTD results. The errors in the resistance for the transmission-line theory are significant (greater than 5%) only when the ratios b/a and $\epsilon_{re}/\epsilon_{ri}$ are both very small. Comparisons were also made for values of the loss tangent higher than one, and the errors in the resonant height and resistance at resonance were found to be comparable to or smaller than for the case $p_e(\omega_{\rm res}) = 1.0$.

V. Conclusions

The FDTD method was used to analyze the insulated linear monopole antenna. The validity of the FDTD analysis was verified by comparison with accurate experimental measurements for the input impedance of the antenna. These measurements are for a wide variety of conditions: bare monopole in air; bare monopole in fresh water and bare monopole in a saline solution, Teflon insulated monopole in air and Teflon insulated monopole in fresh water.

Results from the approximate transmission-line theory for the insulated monopole antenna were compared with results from the FDTD analysis: resonant height and resistance at resonance. These comparisons show that for a lossless external medium, the error in the transmission-line theory can be significant. In particular, the error in the resistance at resonance is greater than 5% when $\epsilon_{re}/\epsilon_{ri} \leq 10$ to 15. The addition of loss to the external medium increases the accuracy of the transmission-line theory. For loss tangents $p_e(\omega_{\rm res}) \geq 1.0$, the error in the resistance at resonance is less than 5%, except when b/a and $\epsilon_{re}/\epsilon_{ri}$ are both very small. Contour plots are provided to quantify the errors as a functions of b/a and $\epsilon_{re}/\epsilon_{ri}$.

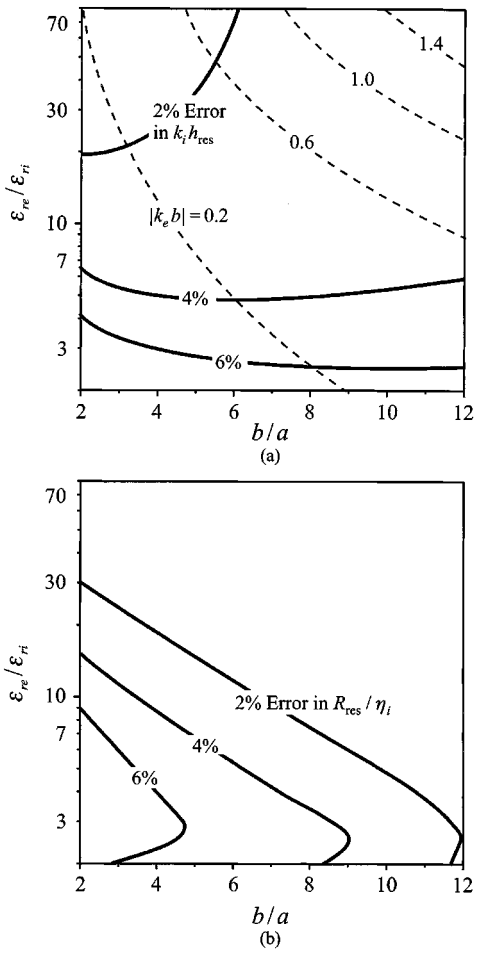

Fig. 7. Contour plot of the error in (a) the resonant height $k_i h_{\rm res}$ and (b) in the resistance at resonance $R_{\rm res}/\eta_i$ as a function of $\epsilon_{re}/\epsilon_{ri}$ and b/a for a lossy external medium $p_e(\omega_{\rm res}) = 1.0$. Lines of constant $|k_e b|$ are dashed on this graph.

Acknowledgment

The authors would like to thank Dr. W. R. Scott, Jr. for sharing his measured results for bare monopole antennas. The authors would also like to thank Dr. J. G. Maloney for helpful discussions of the FDTD analysis and Dr. W. R. Humbert for measuring the permittivity of the Teflon used for the insulated antennas.

References

[1] J. A. Willoughby and P. D. Lowell, "Development of loop aerial for submarine radio communications," *Phys. Rev.*, vol. 14, pp. 193–194, 1919.
[2] R. R. Batcher, "Loop antennas for submarines," *The Wireless Age*, vol. 7, pp. 28–31, 1920.
[3] L. Bouthillon, "Contributions à l'étude des radiocommunications sous-marines," *Rev. Gen. Elect.*, vol. 7, pp. 696–700, 1920.
[4] R. K. Moore, "Theory of radio communication between submerged submarines," Ph.D. dissertation, Cornell Univ., 1951.

[5] ——, "Radio communication in the sea," *IEEE Spectrum*, vol. 4, pp. 42–51, 1967.
[6] R. W. P. King and C. W. Harrison Jr., *Antennas and Waves*. Cambridge, MA: MIT Press, 1969, ch. 6.
[7] R. W. P. King and G. S. Smith, *Antennas in Matter: Fundamentals, Theory, and Applications*. Cambridge, MA: MIT Press, 1981.
[8] J. W. Strohbehn, E. D. Bowers, J. E. Walsh, and E. B. Douple, "An invasive microwave antenna for locally-induced hyperthermia for cancer therapy," *J. Microwave Power*, vol. 14, pp. 339–350, 1979.
[9] D. C. de Sieyes, E. B. Douple, J. W. Strohbehn, and B. S. Trembly, "Some aspects of optimization of an invasive microwave antenna for local hyperthermia treatment of cancer," *Am. Assoc. Phys. Med.*, vol. 8, pp. 174–183, 1981.
[10] R. W. P. King, B. S. Trembly, and J. W. Strohbehn, "The electromagnetic field of an insulated antenna in a conducting or dielectric medium," *IEEE Trans. Microwave Theory Tech.*, vol. MTT-31, pp. 574–583, July 1983.
[11] J. G. Maloney, "Analysis and synthesis of transient antennas using the finite—difference time—domain (FDTD) method," Ph.D. dissertation, Georgia Inst. Technol., 1992.
[12] J. G. Maloney and G. S. Smith, "Modeling of antennas," in *Advances in Computational Electrodynamics: The Finite—Difference Time—Domain Method*, A. Taflove, Ed. Norwood, MA: Artech House, 1998, ch. 7.
[13] J. G. Maloney, M. P. Kesler, and G. S. Smith, "Generalization of PML to cylindrical geometries," in *Proc. 13th Annu. Rev. Progress Appl. Computat. Electromagn.*, 1997, pp. 900–908.
[14] T. W. Hertel, "Pulse radiation from an insulated antenna: An analogue of Cherenkov radiation from a moving charge," M.S. thesis, Georgia Inst. Technol., Atlanta, GA, 1998.
[15] G. S. Smith and W. R. Scott Jr., "The use of emulsion to represent dielectric materials in electromagnetic scale models," *IEEE Trans. Antennas Propagat.*, vol. 38, pp. 323–334, Mar. 1990.
[16] W. R. Scott Jr., "Dielectric spectroscopy using shielded open-circuited coaxial lines and monopole antennas of general length," Ph.D. dissertation, Georgia Inst. Technol., Atlanta, GA, 1985.
[17] W. R. Humbert and W. R. Scott Jr., "Open-structure resonant technique for measuring the dielectric properties of materials," *IEEE Trans. Instrument. Meas.*, vol. 47, pp. 666–673, June 1998.

Thorsten W. Hertel (S'96) was born in Holzminden, Germany, on April 19, 1974. He received the Vordiplom degree in electrical engineering from the Technische Universitaet Braunschweig, Germany, in 1995, and the M.S.E.C.E. degree from the Georgia Institute of Technology, Atlanta, in 1998. He is currently working toward the Ph.D. degree in electrical and computer engineering.

His special interests include numerical modeling with the finite-difference time-domain method and antenna analysis.

Glenn S. Smith (S'65–M'72–SM'80–F'86) received the B.S.E.E. degree from Tufts University, Medford, MA, in 1967, and the S.M. and Ph.D. degrees in applied physics from Harvard University, Cambridge, MA, in 1968 and 1972, respectively.

From 1972 to 1975, he served as a Postdoctoral Research Fellow at Harvard University and also as a part-time Research Associate and Instructor at Northeastern University, Boston, MA. In 1975 he joined the faculty of the School of Electrical and Computer Engineering, Georgia Institute of Technology, Atlanta, where he is currently Regents' Professor and John Pippin Chair of Electromagnetics. He is the author of *An Introduction to Classical Electromagnetic Radiation* (Cambridge, U.K.: Cambridge University Press, 1997) and co-author of *Antennas in Matter: Fundamentals, Theory and Applications* (Cambridge, MA: MIT Press, 1981). He also authored the chapter "Loop Antennas" in *Antenna Engineering Handbook* (New York: McGraw-Hill, 1993). His technical interests include basic electromagnetic theory and measurements, antennas and wave propagation in materials, and the radiation and reception of pulses by antennas.

Dr. Smith is a member of Tau Beta Pi, Eta Kappa Nu, Sigma Xi, and URSI Commissions A and B.